Dephasing of conduction electrons by magnetic impurities in Cu/Ni and Cu/Cr samples: Influence of spin-glass transition on the superconducting proximity effect

I. Sosnin,* P. Nugent, J. Zou, and V. T. Petrashov
Physics Department, Royal Holloway University of London, Egham, Surrey, TW20 0EX, United Kingdom

A. F. Volkov
Theoretische Physik III, Ruhr-Universität Bochum, D-44780 Bochum, Germany
and Institute of Radioengineering and Electronics of the Russian Academy of Sciences, 125009 Moscow, Russia
(Received 6 May 2005; revised manuscript received 1 June 2006; published 20 July 2006)

The dependence of the superconducting proximity effect on the amount of magnetic impurities in the normal part of Andreev interferometers has been studied experimentally. The dephasing rates obtained from fitting experimental data to quasiclassical theory of the proximity effect are consistent with the spin flip scattering from Cr impurities forming a local moment in the Cu host. In contrast, Ni impurities do not form a local moment in Cu and as a result there is no extra dephasing from Ni as long as Cu/Ni alloy remain paramagnetic.

DOI: 10.1103/PhysRevB.74.014511 PACS number(s): 74.45.+c, 72.15.Lh, 72.15.Qm

I. INTRODUCTION

Electron dephasing has been one of the most important problems of mesoscopic physics since its emergence in the 1980s. The main sources of dephasing have been identified as inelastic scattering due to electron-electron and electron-phonon interactions and scattering by magnetic impurities.[1] These have been carefully studied experimentally using the weak localization correction to the conductance of mesoscopic structures.[2] The topic has received renewed interest since the proposal of quantum computing (see, e.g., Ref. 3). Dephasing is one of the major obstacles in building a working solid-state quantum bit. Practically, the phase breaking time τ_ϕ is often limited by the presence of even tiny amounts of magnetic impurities.[4,5]

The mechanism of dephasing by magnetic impurities has been studied extensively using weak localization[6] and the suppression of the superconducting critical temperature.[7] The dephasing rate in these experiments has been identified with the spin-flip rate obtained from the low temperature logarithmic increase in resistivity, the Kondo effect.[8] Theoretically the problem of conductance in mesoscopic systems with magnetic impurities has been studied in various ranges of temperature and impurity concentration.[9–12] Recently, the effect of Kondo impurities on the superconducting proximity effect has been addressed qualitatively in the Au/Fe system.[13]

Here we present an experimental study of the effect of the magnetic impurities on the coherent part of the conductance of a normal metal in proximity to a superconductor. We have investigated a wide range of Kondo temperatures T_K for the two chosen systems $T_K \approx 10$ K for Cu/Cr and $T_K \approx 1000$ K for Cu/Ni.[14] The dephasing rate obtained by fitting amplitude of resistance oscillations with magnetic field to the quasiclassical theory of the proximity effect (see Ref. 15 for a review on the superconducting proximity effect) in both cases is compared to the spin-flip rates estimated from Kondo effect.

II. SAMPLE FABRICATION

The samples were fabricated using *e*-beam lithography and standard processing. The geometry of the structures is shown in Fig. 1. I_1 and I_2 are current leads; V_1 and V_2, are voltage leads. The distance between the N/S contacts is about 150 nm, the length of normal wire between the voltage probes is $L=2.6$ μm. The area of superconducting loop is about 12 μm^2. The first layer was the normal part, 40-nm-thick Cu/Ni or Cu/Cr alloy. The alloy films of various concentrations were fabricated by simultaneous evaporation of Ni or Cr and Cu at fixed rates to obtain the required concentration. To obtain clean interfaces between the layers, the contact area was Ar^+ plasma etched before the deposition of the second (superconducting) layer which was 60-nm-thick Al film. In case of Cu/Ni samples the resulting composition of the film was measured using x-ray spectroscopy in a scanning electron microscope with an accuracy

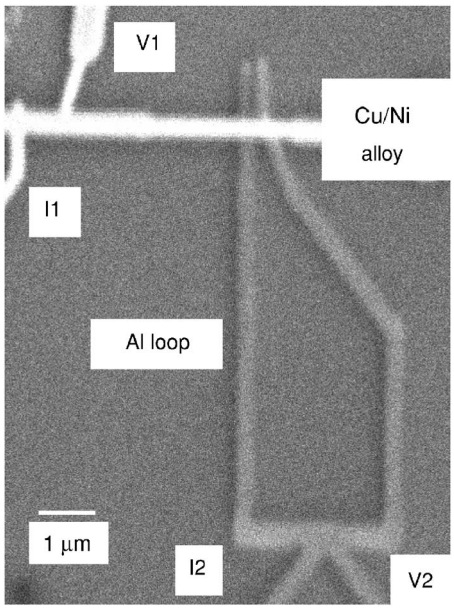

FIG. 1. SEM micrograph of a measured sample. Current contacts are labeled I_1 and I_2; voltage contacts V_1 and V_2. The area of superconducting loop is 12 μm^2.

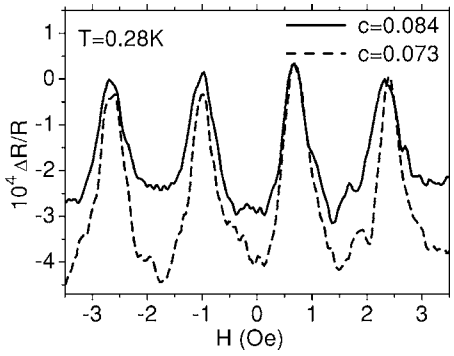

FIG. 2. Magnetoresistance oscillations for two Cu/Ni samples at $T=0.28$ K.

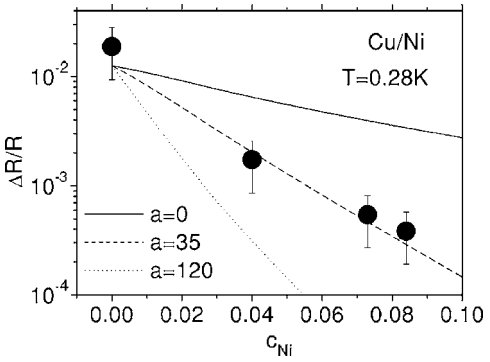

FIG. 3. Dots: Reduced amplitude of resistance oscillations in logarithmic scale as a function of impurity concentration at $T=0.28$ K for Cu/Ni samples. Lines: theoretical fits using $L_{\phi 0}=1.9$ μm and parameter $a=0$ (solid), 35 (dashed), and 120 (dotted).

better than 0.5%. Cr concentration was determined by the slope of logarithmic divergence of resistivity at low temperatures due to the Kondo effect. The homogeneity of the alloy films produced by co-evaporation has been checked by x-ray microanalysis and by dc-extraction magnetometry on ferromagnetic alloys, and was found to be better than 2% (see also 16).

Evaporation sources for alloy film deposition were Cu wire of 99.996% purity and Ni wire of 99.98% purity from Advent, Ltd. Using typical analysis of the source purity provided by the supplier we estimate that up to 10 ppm of other magnetic impurities such as Mn, Cr, or Fe can be introduced into the alloy film during fabrication. Cr source was 99.98% pure from Testbourne, Ltd.

III. EXPERIMENTAL DATA

Two sets of samples have been investigated: Four Cu/Ni samples of geometry shown in Fig. 1 with Ni concentrations 0, 4.0, 7.8, and 8.4 atomic percent and four Cu/Cr samples of similar geometry with Cr concentrations 0, 14, 18, and 41 ppm. All samples showed magnetoresistance oscillations due to the superconducting proximity effect. Figure 2 shows the reduced amplitude of oscillations $\Delta R/R_N$ for two samples with highest Ni concentration (R_N is the resistance of N wire). The period of oscillations corresponds to the magnetic flux quantum $\Phi_0=hc/2e$ through the area of the superconducting loop.

Figure 3 shows the attenuation of reduced amplitude of the proximity effect (in logarithmic scale) with increasing concentration of Ni impurities. Adding up to 8.4 at. % of Ni to Cu suppresses $\Delta R/R_N$ by about 100 times. Dots represent experimental points, while the lines are theoretical fits which will be described later. We estimate the relative inaccuracy in this data to be at least 50% due to uncertainties in sample geometry and the quality of interfaces.

To quantify the effect of Ni impurities on elastic scattering times of conduction electrons we plot the value of residual resistivity at low temperature versus impurity concentration, see Fig. 4. The scattering of experimental values is due to the random amount of disorder introduced during fabrication of thin films. Based on statistics of resistivity measurements we estimate relative inaccuracy of these values to be about 50%. The data allows us to calculate the elastic electron scattering cross section Q_e for Ni impurities using the following relation:[17]

$$Q_e = \frac{e^2}{m v_F} \frac{\partial \rho}{\partial c}, \tag{1}$$

where e is electron charge, m electron mass, v_F is the Fermi velocity, and $c=n_{\mathrm{imp}}/n_{\mathrm{Cu}}$ is the atomic concentration of impurities (n_{imp} and n_{Cu} are concentrations of impurities, Ni or Cr, and Cu atoms, respectively). The data in Fig. 4 gives the experimental slope $\partial\rho/\partial c=0.7$ $\mu\Omega$ cm/at. % in reasonable agreement with 1.3 $\mu\Omega$ cm per at. % of Ni in Cu reported previously.[18] Substituting this value and $v_F=1.6\times10^8$ cm/s (Ref. 19) into Eq. (3) we calculate $Q_e=1.2\times10^{-16}$ cm^2. This allows us to calculate the elastic electron scattering rate on Ni atoms as $\tau_e^{-1}=v_F n_{\mathrm{Cu}} Q_e c$, using $n_{\mathrm{Cu}}=8.45\times10^{22}$ cm^{-3} (Ref. 19).

A small amount of magnetic impurities forming a local moment in the Cu host have been detected by the Kondo effect. The temperature dependence of resistivity in the Cu/Ni alloy wires was measured on separate long lines without any contacts with superconductors made on the same chip simultaneously with the Andreev interferometers. They showed a minimum at temperatures between 3 and 10 K for different concentrations. The position of the minimum corresponds to the Kondo effect due to Fe or Cr impurities. Since Cr has a smaller T_K than Fe does, it will contribute stronger

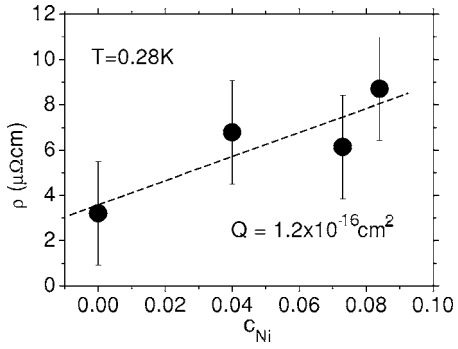

FIG. 4. Dots: Low-temperature residual resistivity vs Ni impurity concentration. Dashed line: best linear fit.

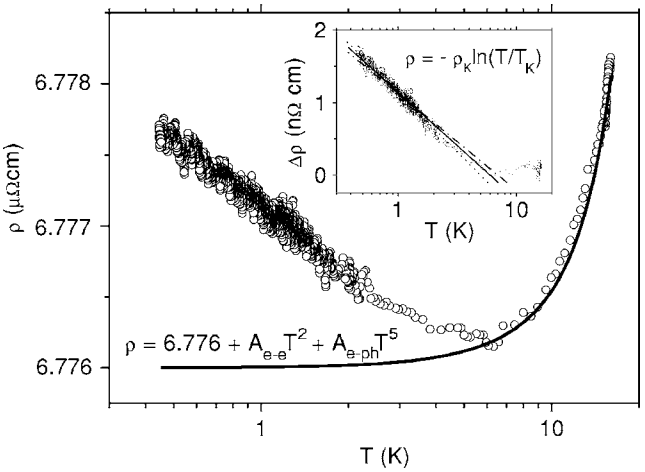

FIG. 5. Circles: Resistivity of Cu+4% Ni sample vs temperature in log scale. Solid line: fit of high-temperature part of resistivity to residual, electron-electron, and electron-phonon contributions. Inset: Kondo contribution to resistivity after subtraction of residual, electron-electron, and electron-phonon contributions. Solid line: best fit to Eq. (2) with ρ_K=0.67 nΩ cm and T_K=6.2 K; dotted line: T_K=5 K; dash-dotted line: T_K=7 K.

to electron dephasing. Figure 5 shows resistivity versus temperature graph for Cu+4% Ni sample. Solid line approximates high-temperature part of resistivity to $\rho=\rho_0+A_{ee}T^2+A_{eph}T^5$, where ρ_0=6.776 μΩ cm is the residual resistivity. After subtracting this fit from the data we fit the remaining dependence to the Kondo formula[8]

$$\Delta\rho = -\rho_K \ln(T/T_K), \tag{2}$$

with two fitting parameters ρ_K and T_K. The inset of Fig. 5 shows the sensitivity of the fit to the values of the Kondo temperature. Our data allows us to estimate T_K within 1 K accuracy. From the slope of the resistivity versus ln T plot we can calculate the concentration of Kondo impurities. For Cr in Cu host the known value is 0.4±0.1 nΩ cm per decade of temperature change per ppm.[20] Figure 6 shows low temperature resistivity increase due to Kondo effect after subtracting electron-electron and electron-phonon contributions for four

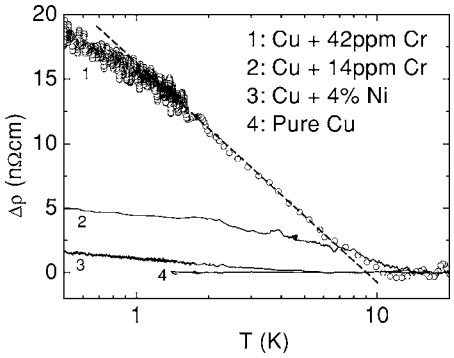

FIG. 6. Resistivity of four samples vs temperature in log scale after subtraction of electron-electron and electron-phonon contributions. Dashed line: Fit to Eq. (2) for sample 1, ρ_K=7.0 nΩ cm and T_K=9.5 K.

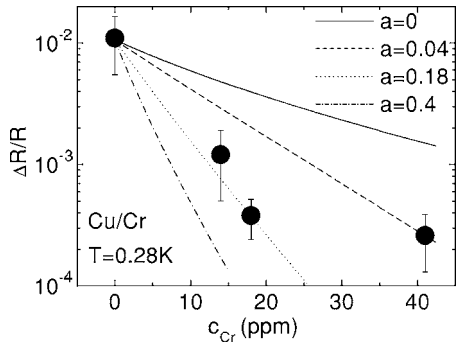

FIG. 7. Dots: Reduced amplitude of resistance oscillations in logarithmic scale as a function of impurity concentration at T =0.28 K for Cu/Cr samples. Lines: theoretical fits using $L_{\phi 0}$ =1.6 μm and parameter a=0 (solid), 0.04 (dashed), 0.18 (dotted), and 0.4 (dash-dotted).

different samples: pure Cu, Cu with 4% Ni, and two Cu/Cr ones. It follows from Fig. 6 that the sample with 4% Ni can contain up to 4 ppm of Cr. Note also similar values of T_K observed in Cu/Ni and Cu/Cr samples. The effect of impurity-impurity interaction is shown in Fig. 6 as deviation at low temperatures from the behavior predicted by Eq. (2) for the sample with 42 ppm of Cr. This may explain the decrease in dephasing rate for the sample with 42 ppm of Cr (see Fig. 7). The pure Cu sample did not show a resistivity minimum which means $c_{Cr}<1$ ppm in our case.

The influence of Cr impurities on the proximity effect is shown in Fig. 7. The dots represent experimentally measured reduced amplitude of magnetoresistance oscillations at T =0.28 K, similar to that shown in Fig. 3 for Cu/Ni samples.

IV. CONDUCTANCE CALCULATION

In order to calculate the correction to the conductance in our structures due to the proximity effect we used Usadel's equation for quasiclassical Green functions induced in the N wire. According to the theory, in the case of a weak superconducting proximity effect, the amplitude of resistance oscillations can be presented as (see, e.g., Ref. 21)

$$\frac{\Delta R(V,T)}{R_N} = \frac{2\int_0^\infty F(\epsilon,V,T)m(\epsilon)d\epsilon}{eV}, \tag{3}$$

where $2V$ is the total voltage applied between the two N reservoirs, ϵ is the quasiparticle energy, $F(V,T)$ is the difference of equilibrium distribution functions in N reservoirs

$$F(V,T) = \frac{\tanh\left(\frac{\epsilon+eV}{2k_BT}\right) - \tanh\left(\frac{\epsilon-eV}{2k_BT}\right)}{2}, \tag{4}$$

and energy-dependent function $m(\epsilon)=(1/16)[m_1(\epsilon)+m_2(\epsilon)+m_3(\epsilon)+m_4(\epsilon)]$ determines averaged over the length (L_1,L) correction to the conductance due to proximity effect. Here $2L$ is the distance between normal reservoirs, $2L_1$ is the distance between N/S contacts, and $L_2=L-L_1$.

$$m_1(\epsilon) = \mathrm{Re}\left[\frac{F_0^2}{\theta^2}\frac{\sinh 2\theta_1 \sinh^2\theta_2 + \sinh 2\theta_2 \sinh^2\theta_1 - 2\theta_1 \sinh^2\theta_2 - 2\theta_2 \sinh^2\theta_1}{2\theta \sinh^2\theta}\right], \tag{5}$$

$$m_2(\epsilon) = \mathrm{Re}\left[\frac{F_0^2}{\theta^2}\frac{2\theta_2 \cosh^2\theta_1 - \sinh 2\theta_2 \cosh^2\theta_1 - 2\theta_1 \sinh^2\theta_2 - \sinh 2\theta_1 \sinh^2\theta_2}{2\theta \cosh^2\theta}\right], \tag{6}$$

$$m_3(\epsilon) = \left|\frac{F_0}{\theta}\right|^2\left[\left|\frac{\sinh\theta_2}{\sinh\theta}\right|^2\left(\frac{\sinh 2\theta_1'}{2\theta'} - \frac{\sin 2\theta_1''}{2\theta''}\right) + \left|\frac{\sinh\theta_1}{\sinh\theta}\right|^2\left(\frac{\sinh 2\theta_2'}{2\theta'} - \frac{\sin 2\theta_2''}{2\theta''}\right)\right], \tag{7}$$

$$m_4(\epsilon) = \left|\frac{F_0}{\theta}\right|^2\left[-\left|\frac{\sinh\theta_2}{\cosh\theta}\right|^2\left(\frac{\sinh 2\theta_1'}{2\theta'} + \frac{\sin 2\theta_1''}{2\theta''}\right) - \left|\frac{\cosh\theta_1}{\cosh\theta}\right|^2\left(\frac{\sinh 2\theta_2'}{2\theta'} - \frac{\sin 2\theta_2''}{2\theta''}\right)\right], \tag{8}$$

where $F_0^2=\Delta^2/[\Delta^2-(\epsilon+i\Gamma)^2]$ is the equilibrium condensate functions in the superconductor, Γ is the depairing rate in the superconductor. Here we neglect the attenuation of condensate functions at the interface because in all our samples R_N was more than 10 times bigger than interface resistance R_{int}. Energy dependence of condensate functions is determined by parameters θ and $\theta_{1,2}$

$$\theta = \theta' + i\theta'' = \sqrt{\frac{2i\epsilon}{E_{\mathrm{Th}}} + \left(\frac{L}{L_\phi}\right)^2}, \tag{9}$$

$\theta_{1,2}=\theta L_{1,2}/L$, $L_\phi=(D\tau_\phi)^{1/2}$ is the phase breaking length in the normal wire and $E_{\mathrm{Th}}=\hbar D/L^2$ is the Thouless energy.

The effect of impurity of concentration c can be included in the model by reducing L_ϕ as follows:

$$\left(\frac{L}{L_{\phi c}}\right)^2 = \left(\frac{L}{L_{\phi 0}}\right)^2(1+bc)(1+ac), \tag{10}$$

where $L_{\phi 0}$ is L_ϕ for pure Cu and $L_{\phi c}$ is L_ϕ at impurity concentration c. Constants b and a describe change in elastic scattering rate and dephasing rate respectively, according to the following linear approximations:

$$\tau_{ec}^{-1} = \tau_{e0}^{-1}(1+bc), \tag{11}$$

$$\tau_{\phi 0c}^{-1} = \tau_{\phi 0}^{-1}(1+ac), \tag{12}$$

where again subscripts "0" and "c" correspond to values for pure Cu and for impurity concentration c. The value of b can be obtained from Fig. 4. Using experimental values for sample parameters and $L_{\phi 0}$ and a as fitting parameters the experimental dependence of proximity effect on impurity concentration can be compared to the one predicted by theory. The value of a is only constant in the single impurity regime. The impurity-impurity interaction leads to the dependence $a=a(c)$. In this way the spin-glass transition can be included in the model as well. This effect is seen for 42 ppm sample in Fig. 5, where the curve obtained in linear approximation does not go through this point.

V. ANALYSIS AND DISCUSSION

Lines in Fig. 3 show results of fitting of experimental data for Cu/Ni samples by the theory as described in Sec. IV. The best fit was obtained for $L_{\phi 0}=1.9$ μm and $a=35$. This corresponds to $\tau_{\phi 0}^{-1}=3.0\times10^9$ s^{-1}. The extra dephasing in Cu/Ni sample with 4% Ni is $\Delta\tau_\phi^{-1}=4.2\times10^9$ s^{-1}. The same calculation for Cu/Cr samples is shown in Fig. 6. The best fit was obtained for $L_{\phi 0}=1.6$ μm and $a=0.18$. This corresponds to $\tau_{\phi 0}^{-1}=7\times10^9$ s^{-1}. The extra dephasing in Cu/Cr sample with 14 ppm of Cr is $\Delta\tau_\phi^{-1}=1.7\times10^{10}$ s^{-1}. Comparing the above two samples one can see that the dephasing in 14 ppm Cr samples is about four times higher than that in 4% Ni sample, and the Kondo slope the former is about 3.5 times higher than that in the former (see Fig. 5). This suggests that the dephasing in Cu/Ni samples can be attributed to the small amount of Cr impurities introduced during Ni deposition. Note that pure Cu samples do not show the Kondo effect within our experimental accuracy, which means that the amount of Cr impurities can be proportional to Ni concentration explaining the dependence of dephasing on concentration of Ni. In our analysis of sources of dephasing we can neglect contributions from electron-phonon interaction which is of the order of 10^6 s^{-1} (Ref. 22) and due to electron-electron interaction which is of the order of 10^8 s^{-1} (Ref. 23) at the temperature of our experiment. Therefore, we assume that additional dephasing is entirely due to magnetic impurities.

For Cu/Ni system impurity spin $S=1/2$ (Ref. 24) so that the spin flip rate in the limit $T\ll T_K$ can be calculated using the following expressions:[12]

$$\tau_{SF}^{-1} = \frac{9\pi^3}{8}\frac{\epsilon_F}{\hbar}\frac{T^2}{T_K^2}\times c, \tag{13}$$

where $\epsilon_F=1.1\times10^{-18}$ J is the Fermi energy of Cu.[18] For 4% Ni sample (13) gives $\tau_{sf}^{-1}=1.4\times10^9$ s^{-1}. This is smaller than the dephasing rate due to Cr impurities.

For Cu/Cr system the spin flip rate at $T<T_K$ can be written as follows:[11]

$$\tau_{SF}^{-1} = 8\pi\frac{\epsilon_F}{\hbar}\frac{S^2-1/4}{\ln^2(T_K/T)}\times c, \tag{14}$$

where $S=3/2$ is Cr impurity spin.[20] The dephasing rate due to spin flip scattering can be found as[11]

$$\tau_\phi^{-1} = \tau_{SF}^{-1} \frac{2}{\left(1 + \frac{\alpha}{2}\frac{T_{SG}}{T}\right)^2}, \quad (15)$$

where $\alpha = 1.85$ for $S = 3/2$ and denominator in right-hand side of Eq. (15) accounts for the reduction of dephasing due to the spin-glass transition at the temperature T_{SG}. Substituting $\tau_\phi^{-1} = 1.7 \times 10^{10}$ s^{-1} for Cu/Cr sample with $c = 14 \times 10^{-6}$ at $T = 0.3$ K into Eqs. (14) and (15) one gets T_{SG} to be about 2 K in reasonable agreement with resistivity measurements shown in Fig. 5.

In conclusion, we have studied the dephasing of conduction electrons by magnetic impurities in Cu/Ni and Cu/Cr samples. Dephasing in Cu/Cr samples is associated with spin-flip scattering due to the Kondo effect. Influence of spin glass transition on the superconducting proximity effect has been observed. Estimation of T_{SG} made using formulas for spin-flip rate and the dephasing rate are in agreement with experiment. The dephasing in Cu/Ni samples can be explained by the contribution of other magnetic impurities, such as Cr by comparison to results in Cu/Cr samples.

ACKNOWLEDGMENTS

We thank L. I. Glazman for valuable discussions. The work was supported by EPSRC Grant No. AF/001343. A.F.V. thanks the DFG for the financial support within the SFB 491 and Mercator-Gastprofessoren.

*Electronic address: i.sosnin@rhul.ac.uk

[1] B. L. Altshuler, A. G. Aronov, and D. E. Khmelnitsky, J. Phys. C **15**, 7367 (1982); D. S. Golubev and A. D. Zaikin, Phys. Rev. Lett. **81**, 1074 (1998).
[2] G. Bergmann, Phys. Rep. **107**, 1 (1984); S. Washburn and R. Webb, Rep. Prog. Phys. **55**, 1311 (1992).
[3] J. Preskill, Phys. Today **52** (6), 24 (1999).
[4] F. Pierre and N. O. Birge, Phys. Rev. Lett. **89**, 206804 (2002).
[5] P. Mohanty and R. A. Webb, Phys. Rev. Lett. **84**, 4481 (2000).
[6] R. P. Peters, G. Bergmann, and R. M. Mueller, Phys. Rev. Lett. **58**, 1964 (1987); C. Van Haesendonck, J. Vranken, and Y. Bruynseraede, *ibid.* **58**, 1968 (1987).
[7] J. A. Chervenak and J. M. Valles, Phys. Rev. B **51**, 11977 (1995).
[8] J. Kondo, Prog. Theor. Phys. **32**, 37 (1964).
[9] V. I. Falko, J. Phys.: Condens. Matter **4**, 3943 (1992).
[10] A. Kaminski and L. I. Glazman, Phys. Rev. Lett. **86**, 2400 (2001).
[11] M. G. Vavilov, L. I. Glazman, and A. I. Larkin, Phys. Rev. B **68**, 075119 (2003).
[12] M. G. Vavilov and L. I. Glazman, Phys. Rev. B **67**, 115310 (2003).
[13] J. Eom, J. Aumentado, V. Chandrasekhar, P. M. Baldo, and L. E. Rehn, Solid State Commun. **127**, 545 (2003).
[14] M. D. Daybell and W. A. Steyert, Rev. Mod. Phys. **40**, 380 (1968).
[15] C. J. Lambert and R. Raimondi, J. Phys.: Condens. Matter **10**, 901 (1998).
[16] P. Nugent, I. Sosnin, and V. T. Petrashov, J. Phys.: Condens. Matter **16**, L509 (2004).
[17] A. A. Abrikosov, *Fundamentals of the Theory of Metals* (North Holland, Amsterdam, 1988).
[18] P. A. Schroeder, R. Wolf, and J. A. Woollam, Phys. Rev. **138**, A105 (1965).
[19] C. Kittel, *Introduction to Solid State Physics* (Wiley, New York, 1971).
[20] M. D. Daybell and W. A. Steyert, Phys. Rev. Lett. **18**, 398 (1967); M. D. Daybell and W. A. Steyert, *ibid.* **20**, 195 (1968).
[21] A. F Volkov, N. Alsopp, and C. J. Lambert, J. Phys.: Condens. Matter **8**, L45 (1996); V. T. Petrashov, R. Sh. Shaikhaidarov, I. A. Sosnin, P. Delsing, T. Claeson, and A. Volkov, Phys. Rev. B **58**, 15088 (1998).
[22] D. P. Love, C. T. Van Degrift, and W. H. Parker, Phys. Rev. B **26**, 5577 (1982).
[23] J. F. Koch and R. E. Doezema, Phys. Rev. Lett. **24**, 507 (1970).
[24] G. Khaliullin, R. Kilian, S. Krivenko, and P. Fulde, cond-mat/9810032 (unpublished); V. Madhavan, T. Jamneala, K. Nagaoka, W. Chen, J.-L. Li, S. G. Louie, and M. F. Crommie, Phys. Rev. B **66**, 212411 (2002).